

# Thermal displacement by marine heatwaves

<https://doi.org/10.1038/s41586-020-2534-z>

Michael G. Jacox<sup>1,2,3</sup>✉, Michael A. Alexander<sup>2</sup>, Steven J. Bograd<sup>1,3</sup> & James D. Scott<sup>2,4</sup>

Received: 28 January 2020

Accepted: 15 June 2020

Published online: 5 August 2020

 Check for updates

Marine heatwaves (MHWs)—discrete but prolonged periods of anomalously warm ocean temperatures—can drastically alter ocean ecosystems, with profound ecological and socioeconomic impacts<sup>1–8</sup>. Considerable effort has been directed at understanding the patterns, drivers and trends of MHWs globally<sup>9–11</sup>. Typically, MHWs are characterized on the basis of their intensity and persistence at a given location—an approach that is particularly relevant for corals and other sessile organisms that must endure increased temperatures. However, many ecologically and commercially important marine species respond to environmental disruptions by relocating to favourable habitats, and dramatic range shifts of mobile marine species are among the conspicuous impacts of MHWs<sup>1,4,12,13</sup>. Whereas spatial temperature shifts have been studied extensively in the context of long-term warming trends<sup>14–18</sup>, they are unaccounted for in existing global MHW analyses. Here we introduce thermal displacement as a metric that characterizes MHWs by the spatial shifts of surface temperature contours, instead of by local temperature anomalies, and use an observation-based global sea surface temperature dataset to calculate thermal displacements for all MHWs from 1982 to 2019. We show that thermal displacements during MHWs vary from tens to thousands of kilometres across the world's oceans and do not correlate spatially with MHW intensity. Furthermore, short-term thermal displacements during MHWs are of comparable magnitude to century-scale shifts inferred from warming trends<sup>18</sup>, although their global spatial patterns are very different. These results expand our understanding of MHWs and their potential impacts on marine species, revealing which regions are most susceptible to thermal displacement, and how such shifts may change under projected ocean warming. The findings also highlight the need for marine resource management to account for MHW-driven spatial shifts, which are of comparable scale to those associated with long-term climate change and are already happening.

Over the past decade, the marine research community has been galvanized by a series of high-profile MHWs with extensive impacts on marine ecosystems, as well as the communities and economies that these ecosystems support<sup>1,2,5,7,8,19,20</sup>. In assessing such events, MHWs have been defined and characterized on the basis of the local amplitude and persistence of sea surface temperature (SST) anomalies<sup>21</sup>, an approach that draws on similar definitions for atmospheric heatwaves<sup>22</sup>. However, although temporary relocation is generally not a feasible solution to heatwave impacts over land (for example, on infrastructure, agriculture and human health), mobile marine species (for example, many fishes and marine mammals) can shift their distributions to find a preferred habitat, and in some cases track ocean temperature with little to no lag<sup>16,17</sup>. Despite the fact that marine species respond in different ways to a wide variety of physical, chemical and biological drivers and cues, relatively simple SST-based habitat metrics have proven informative for understanding species redistributions under environmental change<sup>14,16,17,23</sup>. To account for this critical dimension of MHW impacts, which is not captured by local temperature anomaly metrics, we introduce and quantify the 'thermal displacement' associated with MHWs

across the globe. Thermal displacement is the minimum distance that must be travelled away from an MHW to track constant SST. It is related to climate velocity (the rate at which isotherms move across the Earth's surface under climate change<sup>18</sup>) but is applied on an event scale in which the magnitude of the displacement, not the rate of change, is of greatest interest. Here, we use monthly SST anomalies from version 2 of the NOAA 0.25° Optimum Interpolation SST product to explore historical (1982–2019) spatial and temporal patterns of thermal displacement throughout the world's oceans, and then quantify the future change in these displacements associated with projected warming from an ensemble of climate models.

On a global scale, MHW intensity is spatially heterogeneous<sup>9,11</sup>, with typical SST anomalies ranging from under 1 °C (for example, in the tropical Indian and Atlantic Oceans) to about 4 °C in the Eastern Tropical Pacific and in the vicinity of energetic midlatitude currents and their associated fronts (Fig. 1a, b). Thermal displacement also varies considerably in space, exhibiting a difference of two orders of magnitude (from tens to thousands of kilometres) across the world's oceans (Fig. 1c, Extended Data Fig. 1). The global median thermal displacement

<sup>1</sup>NOAA Southwest Fisheries Science Center, Monterey, CA, USA. <sup>2</sup>NOAA Earth System Research Laboratory, Boulder, CO, USA. <sup>3</sup>University of California Santa Cruz, Santa Cruz, CA, USA.

<sup>4</sup>University of Colorado, Boulder, CO, USA. ✉e-mail: michael.jacox@noaa.gov

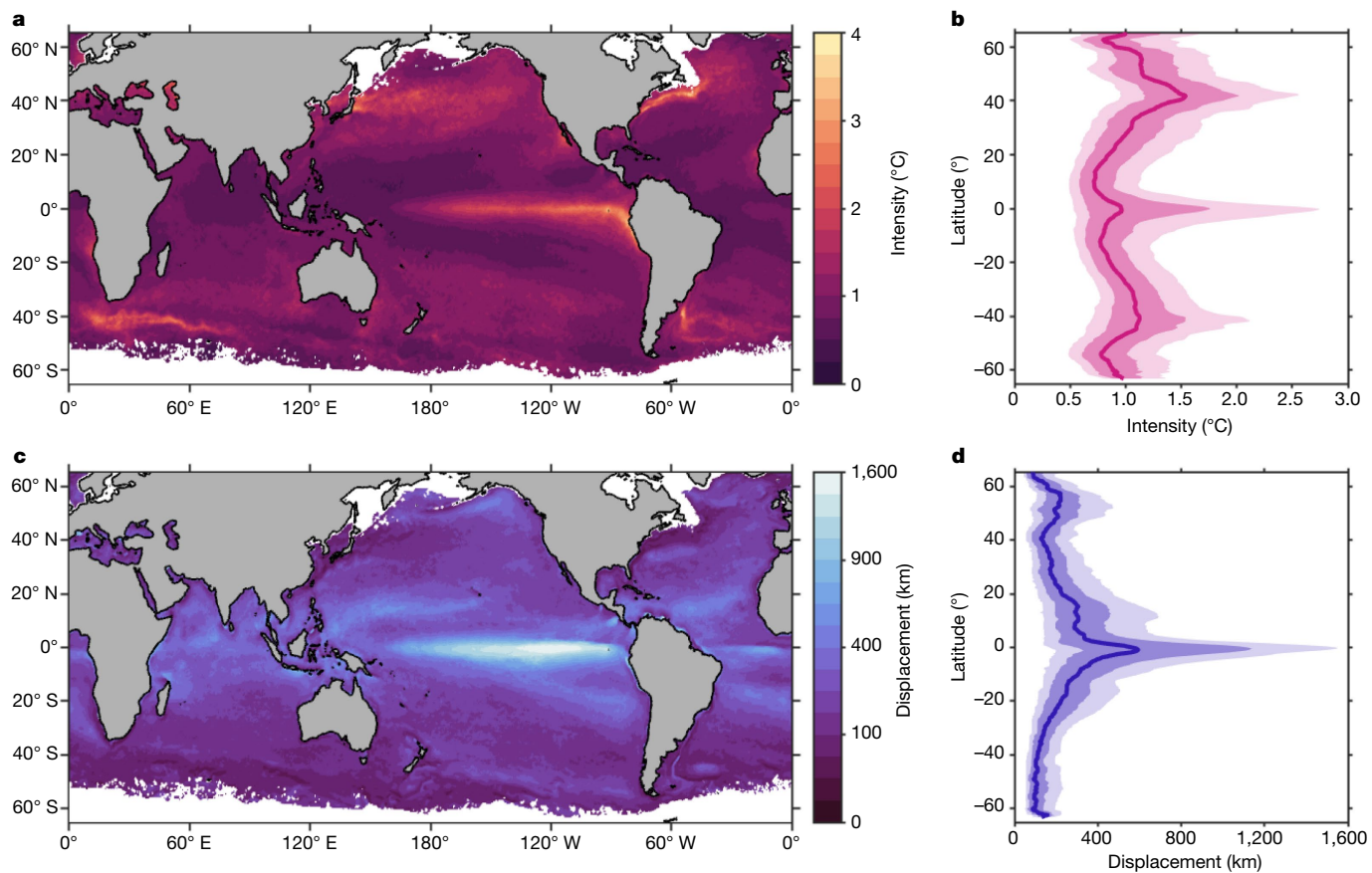


**Fig. 1 | MHWs and their influence on thermal habitat redistribution globally.** **a**, Median MHW intensity (the SST anomaly associated with an MHW) from 1982 to 2019, calculated at each grid cell from all months with an active MHW. **c**, Median thermal displacement associated with MHWs. Thermal displacements can be in any direction (see Methods). White regions have

seasonal or permanent sea ice cover. **b, d**, Zonal median values of MHW intensity and thermal displacement, with bands indicating the 25th–75th and 10th–90th percentile ranges. Medians and percentiles are used instead of means and variance because MHW metric distributions are skewed to the right (Extended Data Fig. 1).

associated with MHWs, calculated over the ice-free regions of the ocean, is 183 km. For reference, the global median shift associated with historical ocean warming trends has been estimated as 21.7 km per decade<sup>18</sup>. Peaks in MHW intensity are evident near the Equator and in the midlatitudes (centred on  $\sim 40^{\circ}$  N and  $\sim 40^{\circ}$  S) and thermal displacement is greatest near the Equator. For both MHW intensity and thermal displacement, higher magnitude is also associated with higher variance (Fig. 1, Extended Data Fig. 2). Although MHW intensity and thermal displacement are aligned in some regions (the Eastern Tropical Pacific stands out for its high values of both metrics due to El Niño events), they have little spatial correlation globally (Spearman rank correlation  $r = -0.27$ ; Extended Data Fig. 3). In fact, some of the regions that are most susceptible to intense MHWs, particularly in western boundary current extensions and the Antarctic Circumpolar Current, are also characterized by very small thermal displacements (Fig. 1). However, temporal variability in thermal displacement does correlate with MHW intensity over much of the global ocean, although the Northwestern Atlantic and Northwestern Pacific oceans are notable exceptions (Extended Data Fig. 4).

Spatial patterns in thermal displacement are strongly influenced by the spatial structure of the mean SST field. The SST gradient determines what distance must be covered to compensate for a given SST anomaly, with weaker gradients translating to longer distances ( $r = -0.81$ ; Fig. 1, Extended Data Fig. 3; ref.<sup>18</sup>). The most dramatic thermal displacements generally occur in regions of very weak SST gradients, particularly tropical oceans, where displacements reach upwards of 500 km per degree of SST anomaly (Fig. 2). In areas where MHWs are intense and

occur on a backdrop of very weak SST gradients (particularly the Eastern Tropical Pacific), thermal displacements can exceed 2,000 km. Conversely, in regions of strong SST gradients, colder water is generally not far away; although shifts in strong ocean currents and the associated gradients can quickly generate large SST anomalies, those anomalies do not translate to large thermal displacements (for example, in the Gulf Stream and Antarctic Circumpolar Current; Fig. 2). A special case arises for cold refugia; although these regions may be characterized by strong SST gradients, they are surrounded by warmer water. As a result, MHWs occurring in cold refugia can be particularly impactful in terms of thermal displacement (for example, in the California and Humboldt current systems; Fig. 2). In some cases, MHWs can alter the surface temperature field so that the thermal habitat is not accessible at all, particularly in inland seas and in regions bounded by land in the poleward direction.

Several MHWs have received extensive scientific and public attention in the past decade, and can be viewed through the lens of thermal displacement. In the Northeast Pacific, 2014–2016 brought an unprecedented MHW initially situated offshore ('the Blob')<sup>20</sup> that later evolved into an arc warming pattern spanning the North American west coast<sup>24</sup>. During this event, thermal displacements exceeded 700 km in the Gulf of Alaska and along the US west coast. Similar displacements were generated in 2005 by the delayed upwelling season and consequent warming<sup>25,26</sup> (Fig. 3a). The 2012 Northwest Atlantic MHW<sup>1,27</sup> was the most intense seen in the region in 30 years, and drove commercially valuable species to rapidly shift poleward by hundreds of kilometres<sup>1</sup>. Although species shifts are not driven purely by surface temperature,

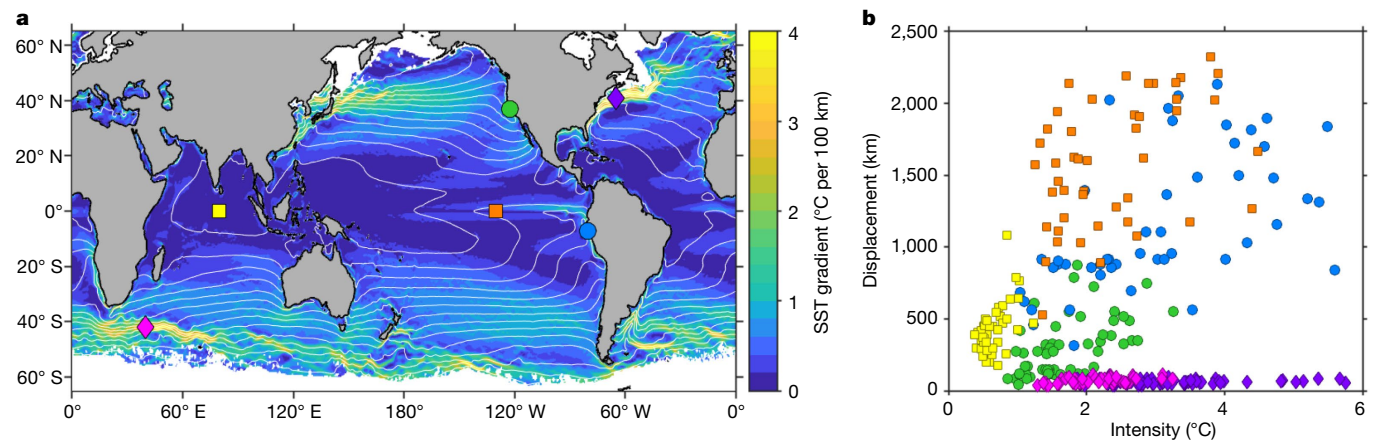


**Fig. 2 | Dependence of thermal displacement on MHW intensity and background SST gradients.** **a**, Horizontal SST gradients (colour) and mean SST (contours ranging 2–28 °C at 2 °C intervals), with sample locations indicated by coloured markers. **b**, Thermal displacement as a function of monthly MHW intensity for all MHWs from 1982 to 2019 in six sample regions,

characterized by strong SST gradients (diamonds; Gulf Stream: purple, Antarctic Circumpolar Current: pink), weak SST gradients (squares; Tropical Indian Ocean: yellow, Eastern Tropical Pacific: orange) and coastal upwelling that provides cold refugia (circles; California Current System: green, Humboldt Current System: blue).

they were consistent with calculated thermal displacements for that event (Fig. 3b). Given the complex political geography of the eastern seaboard of the United States, this event highlighted management questions introduced by MHW-driven shifts across state and national lines<sup>1</sup>. Along Australian coasts, the 2010s brought repeated MHWs, including in 2010–2011 off Western Australia<sup>2,19</sup>, in 2015–2016 in the Tasman Sea<sup>8</sup> and in 2016 off the northern coast<sup>5</sup>. However, mean SST gradients are generally strong and meridionally oriented in Australian seas (Fig. 2), with resultant thermal displacements that are relatively small (Fig. 3c). Lastly, El Niño events have caused some of the largest

thermal displacements globally; during the 2015–2016 event, they exceeded 2,000 km in the Eastern Tropical Pacific, an impact matched by that of the 1997–1998 El Niño event (Fig. 3d), during which large poleward shifts of marine fishes were observed along both the North and South American west coasts<sup>12,28,29</sup>.

Spatial shifts in climate driven by warming trends, and the resultant changes in species distributions, have been studied extensively in terrestrial and marine systems<sup>14,16–18,30</sup>. However, changes in the variability around those long-term shifts (for example, due to MHWs) have received little attention. Future ocean warming is projected to be

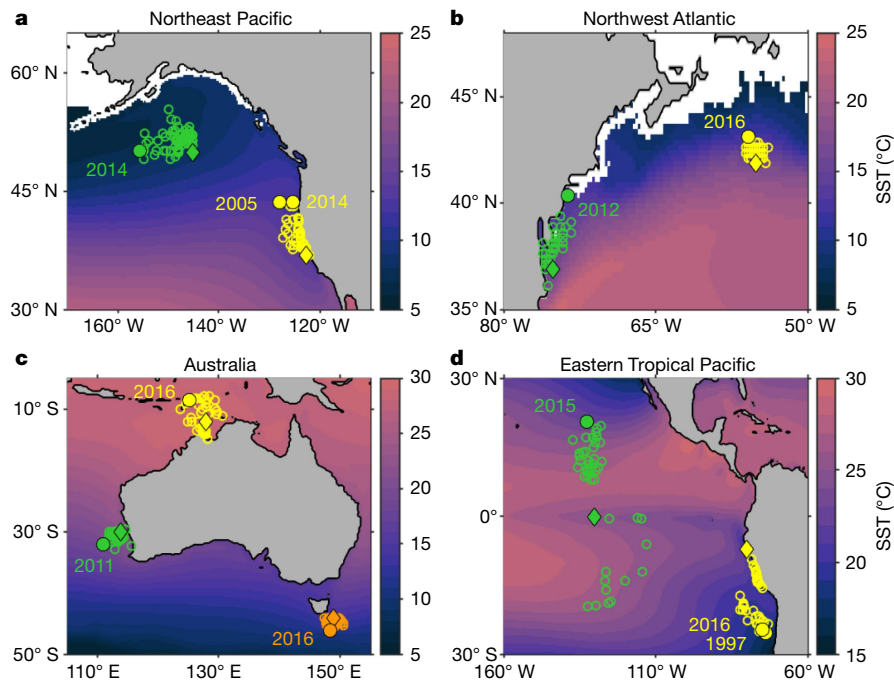


**Fig. 3 | Thermal displacements for select locations subject to notable MHWs.** **a–d**, For each region, displacements from select locations (diamonds) are shown for all months with an active MHW from 1982 to 2019 (open circles). Displacements and years of prominent MHWs are also shown for each location (filled circles). For the South American west coast (**d**), displacements for the 1997 and 2016 MHWs are almost entirely overlapping. Spatial scales differ between panels. For reference, displacement distances for labelled events are:

in **a**, 750 km (Gulf of Alaska, 2014), 872 km and 786 km (US West Coast, 2005 and 2014, respectively); in **b**, 410 km and 152 km (Northwest Atlantic, 2012 and 2016, respectively); in **c**, 362 km (Western Australia, 2011), 492 km (Northern Australia, 2016) and 226 km (Tasman Sea, 2016); and in **d**, 2,323 km (Eastern Tropical Pacific, 2015), 2,135 km and 2,025 km (South American West Coast, 1997 and 2016, respectively). The background colour indicates the mean SST in 1982–2019.

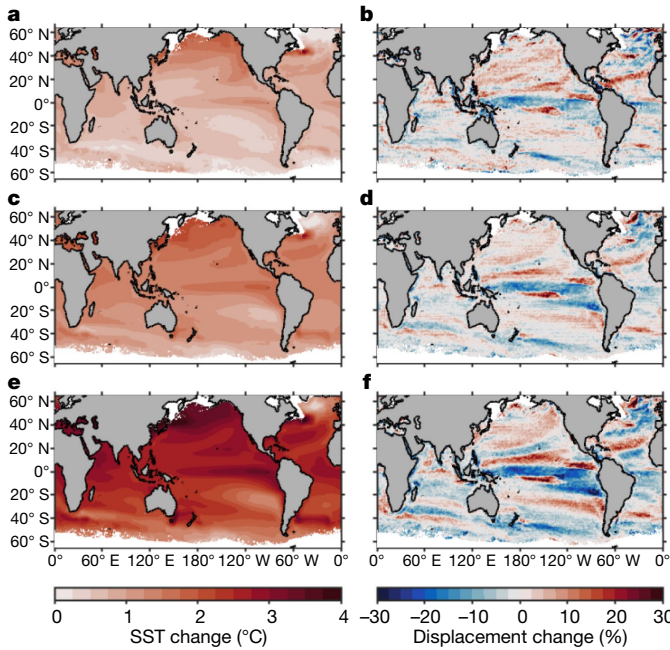


**Fig. 4 | SST and thermal displacement changes under projected 21<sup>st</sup>-century warming.** a, c, e, Mean SST changes from the historical reference period (1982–2011) to the end of the century (2070–2099) calculated using the fifth Coupled Model Intercomparison Project ensemble (CMIP5) are shown for RCP2.6 (a), RCP4.5 (c) and RCP8.5 (e). Changes in median MHW thermal displacement between the same two periods, each calculated relative to its contemporaneous climatology, are shown for RCP2.6 (b), RCP4.5 (d) and RCP8.5 (f).

spatially heterogeneous (Fig. 4), which will intensify SST gradients in some regions and weaken them in others. Consequently, thermal displacements during MHWs will be altered even if interannual SST variability is unchanged. Given the mean projected warming by the late 21<sup>st</sup> century (2070–2099) under the RCP8.5 scenario, these changes reach ~30% of the historical thermal displacements (as much as several hundred kilometres depending on the region affected) and can be of either sign, which means that discrete regions may become more or less vulnerable to short-term thermal displacements. In lower-emissions scenarios (RCP2.6 and RCP4.5), thermal displacement changes are smaller but show the same spatial patterns (Fig. 4). In general, thermal displacement by MHWs will tend to increase under future warming in regions with decreased horizontal gradients; such is the case for much of the North Pacific, where intensified warming in the subarctic region is projected. The opposite is true for much of the Northeast Atlantic and Southern oceans, where warming is projected to be relatively weak at higher latitudes (Fig. 4b). The changes described here for MHW displacements will occur on top of long-term temperature trends, and understanding both of these factors is crucial<sup>31</sup> as their regional signatures will be different. For example, relatively strong projected warming along the equatorial Pacific would drive large long-term thermal shifts, but would also intensify meridional SST gradients and thereby reduce thermal displacement during future MHWs (although it should be noted that the accuracy of climate models for the tropical Pacific SST response to global warming has been called into question)<sup>32</sup>. Similarly, species shifting to new areas in response to long-term temperature trends will probably also experience changes in MHW-driven thermal displacements relative to those at their current locations.

Shifting species distributions must be accounted for in fisheries management<sup>33</sup>, as species' range shifts take them across management boundaries, alter their proximity to fishing ports and drive the need

for adaptive measures by fishing communities<sup>34</sup>. Fisheries follow shifting species distributions, although the response is lagged, at least in part, owing to economic and regulatory constraints<sup>35</sup>. These management issues are often discussed in the context of climate change<sup>23</sup>, but because of the rapid disturbance introduced by MHWs and other transient events, they need to be addressed now. Modern-day MHWs can induce thermal displacements comparable to those resulting from century-scale warming trends and although these temperature shifts alone do not dictate species distributions, they do convey the scale of potential habitat disruption. Furthermore, whereas MHWs themselves are transient events, with many species likely to return following a temporary displacement, in some cases the habitat shifts imparted by MHWs may trigger lasting ecological change as species gain access to previously unavailable habitat or lose access to previously available habitat (that is, through ecological bridges and barriers<sup>36</sup>). Thus, it is crucial that resource management considers shifts in oceanographic habitat not only in the context of secular change but also relative to extreme events now and under future climatic conditions.

The utility of mapping thermal shifts to inform our understanding of ecological responses has been thoroughly demonstrated<sup>14,16,17,23</sup>. However, thermal displacement remains a simplistic proxy for potential changes in the distributions of marine species. We anticipate that our analysis will be expanded upon for individual (or groups of) species by incorporating additional considerations, including vertical movements, physiology, additional essential habitat properties, such as prey and oxygen, and other restrictions on species distributions (for example, the need to be near shore or specific breeding or nursing grounds). Such analyses can further constrain whether areas of suitable temperature are actually viable habitat and, if not, where suitable habitat may be available. Thermal displacement should also be considered in conjunction with previously introduced MHW metrics, including intensity and duration, given that the amplitude and persistence of temperature anomalies relative to species' tolerances will dictate whether these species can remain in place or need to relocate to find favourable conditions<sup>37</sup>. Characterizing MHWs by their thermal displacement, in addition to these other metrics, offers a new perspective on the spatial imprint of MHWs across the globe and their potential impacts on mobile marine species and the communities that depend on them.

## Online content

Any methods, additional references, Nature Research reporting summaries, source data, extended data, supplementary information, acknowledgements, peer review information; details of author contributions and competing interests; and statements of data and code availability are available at <https://doi.org/10.1038/s41586-020-2534-z>.

1. Mills, K. et al. Fisheries management in a changing climate: lessons from the 2012 ocean heat wave in the Northwest Atlantic. *Oceanography* **26**, 191–195 (2013).
2. Wernberg, T. et al. An extreme climatic event alters marine ecosystem structure in a global biodiversity hotspot. *Nat. Clim. Chang.* **3**, 78–82 (2013).
3. Thomsen, J. A. et al. Extreme temperatures, foundation species, and abrupt ecosystem change: an example from an iconic seagrass ecosystem. *Glob. Change Biol.* **21**, 1463–1474 (2015).
4. Cavole, L. M. et al. Biological impacts of the 2013–2015 warm-water anomaly in the Northeast Pacific: winners, losers, and the future. *Oceanography* **29**, 273–285 (2016).
5. Hughes, T. P. et al. Global warming and recurrent mass bleaching of corals. *Nature* **543**, 373–377 (2017).
6. Babcock, R. C. et al. Severe continental-scale impacts of climate change are happening now: extreme climate events impact marine habitat forming communities along 45% of Australia's coast. *Front. Mar. Sci.* **6**, 411 (2019); corrigendum **6**, 558 (2019).
7. Smale, D. A. et al. Marine heatwaves threaten global biodiversity and the provision of ecosystem services. *Nat. Clim. Chang.* **9**, 306–312 (2019).
8. Oliver, E. C. et al. The unprecedented 2015/16 Tasman Sea marine heatwave. *Nat. Commun.* **8**, 16101 (2017).
9. Oliver, E. C. et al. Longer and more frequent marine heatwaves over the past century. *Nat. Commun.* **9**, 1324 (2018).
10. Frölicher, T. L., Fischer, E. M. & Gruber, N. Marine heatwaves under global warming. *Nature* **560**, 360–364 (2018).
11. Holbrook, N. J. et al. A global assessment of marine heatwaves and their drivers. *Nat. Commun.* **10**, 2624 (2019).

12. Ñiquen, M. & Bouchon, M. Impact of El Niño events on pelagic fisheries in Peruvian waters. *Deep Sea Res. Part II* **51**, 563–574 (2004).
13. Walker, H. J. et al. Unusual occurrences of fishes in the southern California current system during the warm water period of 2014–2018. *Estuar. Coast. Shelf Sci.* **236**, 106634 (2020).
14. Perry, A. L., Low, P. J., Ellis, J. R. & Reynolds, J. D. Climate change and distribution shifts in marine fishes. *Science* **308**, 1912–1915 (2005).
15. Sorte, C. J., Williams, S. L. & Carlton, J. T. Marine range shifts and species introductions: comparative spread rates and community impacts. *Glob. Ecol. Biogeogr.* **19**, 303–316 (2010).
16. Pinsky, M. L., Worm, B., Fogarty, M. J., Sarmiento, J. L. & Levin, S. A. Marine taxa track local climate velocities. *Science* **341**, 1239–1242 (2013).
17. Poloczanska, E. S. et al. Global imprint of climate change on marine life. *Nat. Clim. Chang.* **3**, 919–925 (2013).
18. Burrows, M. T. et al. The pace of shifting climate in marine and terrestrial ecosystems. *Science* **334**, 652–655 (2011).
19. Pearce, A. F. & Feng, M. The rise and fall of the “marine heat wave” off Western Australia during the summer of 2010/2011. *J. Mar. Syst.* **111–112**, 139–156 (2013).
20. Bond, N. A., Cronin, M. F., Freeland, H. & Mantua, N. Causes and impacts of the 2014 warm anomaly in the NE Pacific. *Geophys. Res. Lett.* **42**, 3414–3420 (2015).
21. Hobday, A. J. et al. A hierarchical approach to defining marine heatwaves. *Prog. Oceanogr.* **141**, 227–238 (2016).
22. Perkins, S. E. & Alexander, L. V. On the measurement of heat waves. *J. Clim.* **26**, 4500–4517 (2013).
23. Brito-Morales, I. et al. Climate velocity can inform conservation in a warming world. *Trends Ecol. Evol.* **33**, 441–457 (2018).
24. Di Lorenzo, E. & Mantua, N. Multi-year persistence of the 2014/15 North Pacific marine heatwave. *Nat. Clim. Chang.* **6**, 1042–1047 (2016).
25. Schwing, F. B. et al. Delayed coastal upwelling along the US West Coast in 2005: a historical perspective. *Geophys. Res. Lett.* **33**, L22S01 (2006).
26. Brodeur, R. D. et al. Anomalous pelagic nekton abundance, distribution, and apparent recruitment in the northern California Current in 2004 and 2005. *Geophys. Res. Lett.* **33**, L22S08 (2006).
27. Chen, K., Gawarkiewicz, G. G., Lentz, S. J. & Bane, J. M. Diagnosing the warming of the northeastern US coastal ocean in 2012: a linkage between the atmospheric jet stream variability and ocean response. *J. Geophys. Res.* **119**, 218–227 (2014).
28. Lea, R. N. & Rosenblatt, R. H. Observations on fishes associated with the 1997–98 El Niño off California. *Cal. Coop. Ocean. Fish.* **41**, 117–129 (2000).
29. Pearcey, W. G. Marine nekton off Oregon and the 1997–98 El Niño. *Prog. Oceanogr.* **54**, 399–403 (2002).
30. Loarie, S. R. et al. The velocity of climate change. *Nature* **462**, 1052–1055 (2009).
31. Jacox, M. G. Marine heatwaves in a changing climate. *Nature* **571**, 485–487 (2019).
32. Seager, R. et al. Strengthening tropical Pacific zonal sea surface temperature gradient consistent with rising greenhouse gases. *Nat. Clim. Chang.* **9**, 517–522 (2019).
33. Link, J. S., Nye, J. A. & Hare, J. A. Guidelines for incorporating fish distribution shifts into a stock assessment context. *Fish Fish.* **12**, 461–469 (2011).
34. Rogers, L. A. et al. Shifting habitats expose fishing communities to risk under climate change. *Nat. Clim. Chang.* **9**, 512–516 (2019).
35. Pinsky, M. L. & Fogarty, M. Lagged social-ecological responses to climate and range shifts in fisheries. *Clim. Change* **115**, 883–891 (2012).
36. Briscoe, D. K. et al. Ecological bridges and barriers in pelagic ecosystems. *Deep Sea Res. Part II* **140**, 182–192 (2017).
37. Sunday, J. M. et al. Species traits and climate velocity explain geographic range shifts in an ocean-warming hotspot. *Ecol. Lett.* **18**, 944–953 (2015).

**Publisher's note** Springer Nature remains neutral with regard to jurisdictional claims in published maps and institutional affiliations.

© The Author(s), under exclusive licence to Springer Nature Limited 2020

## Methods

### Defining marine heatwaves

Historical SST observations for the 1982–2019 period were obtained from the NOAA 0.25° Optimum Interpolation SST, version 2 (OISSTv2<sup>38,39</sup>), which has been used previously for MHW detection<sup>9</sup>. We masked out regions where OISSTv2 ice concentrations were greater than zero for more than 15 days in a month. MHWs were identified on the basis of methodology adapted from Hobday et al.<sup>21</sup>. For each grid cell we calculated time series of SST anomalies relative to the 1982–2011 climatology and classified MHWs as periods with SST anomalies above a seasonally varying 90th-percentile threshold (Extended Data Fig. 5). Our analysis differs from those used in some other studies in that we used monthly averaged SST rather than daily data, and we detrended the SST anomalies to distinguish discrete, transient MHWs from the long-term warming signal<sup>31</sup>. Although we believe that the choices to use monthly data and to detrend anomalies are the most appropriate for this analysis, we are aware of the lack of consensus on these aspects of MHW definition and detection. Therefore, in section ‘Justification for MHW definition and implications for this study’ we outline the motivations for our choices and we compare our results to those based on daily data and those calculated without removing the warming trend. Neither the monthly data frequency nor the detrending qualitatively affect our results.

### Calculating thermal displacement

For each MHW (that is, every month characterized as an MHW in each grid cell), the climatological SST ( $SST_{CLIM}$ ) for that location and time was first determined by subtracting the detrended SST anomaly from the observed SST. Thermal displacement was then calculated as the great circle distance to the nearest grid cell with SST equal to or less than  $SST_{CLIM}$  (Extended Data Fig. 5). Thermal displacements were constrained so that unrealistic paths through land barriers (for example, entering or exiting inland seas, crossing continents between ocean basins) did not alter the large-scale patterns presented here. However, paths that interacted with land were allowed if they represented realistic displacements (for example, along the California coast in Fig. 3a); in such cases, the reported thermal displacements underestimate the true distance travelled by an oceanic pathway. Regions for which a displaced thermal habitat is sometimes unreachable include inland seas as well as gulfs, bays, and seas that are bounded by land masses on the poleward side. We note that an alternative approach drawing on the climate velocity literature would be to calculate the thermal displacement as the MHW intensity divided by the local SST gradient. This approach is appropriate for climate velocity, a local rate of change, but fails for MHW-driven thermal displacements that depend not only on the local SST gradient but also on the broader spatial structure of SST and locations of land masses.

### Future change

Projected global SST changes were calculated using historical and multiple future scenarios from coupled atmosphere–ocean models included in the fifth Coupled Model Intercomparison Project (CMIP5). For the highest-emissions scenario, RCP8.5, model output was obtained for 28 models: ACCESS1-0, ACCESS1-3, CANESM2, CCSM4, CESM1-BGC, CESM1-CAM5, CMCC-CESM, CMCC-CM, CNRM-CM5, CSIRO-MK3-6-0, GFDL-CM3, GFDL-ESM2G, GFDL-ESM2M, GISS-E2-H, GISS-E2-R, HADGEM2-AO, HADGEM2-CC, HADGEM2-ES, INMCM4, IPSL-CM5A-LR, IPSL-CM5A-MR, IPSL-CM5B-LR, MIROC5, MIROC-ESM, MPI-ESM-LR, MPI-ESM-MR, NORESM1-ME and NORESM1-M (for more information, see <https://www.esrl.noaa.gov/psd/ipcc/cmip5/models.html>). For the moderate-emissions RCP4.5 scenario, output was obtained from the same models, except for CMCC-CESM. For the lowest-emissions scenario, RCP2.6, output was available from just seven of these models: CANESM2, HADGEM2-AO, MIROC-ESM, MIROC-ESM-CHEM, MIROC5,

MPI-ESM-LR and MPI-ESM-MR. SST output from each model was bilinearly interpolated to a common  $1^\circ \times 1^\circ$  grid before creating an ensemble-average SST. The future change was defined as the difference between monthly mean climates of historical (1982–2011) and future (2070–2099) periods. Month-dependent changes from the CMIP5 ensemble were interpolated to the OISST grid with a cubic interpolation and added to the observed 1982–2019 OISSTv2 data to produce future SST fields at the 0.25° OISST resolution. We then repeated the steps described in section ‘Calculating thermal displacement’ and in Extended Data Fig. 5 to identify MHWs and thermal displacements for the future period as we did for the historical period. Because we analyse the future period by adding the mean projected change to the historical time series, the interannual variability of the historical observations is retained, and the phase (that is, interannual to decadal variability) of individual climate model realizations does not affect our results. Thus, the reported changes in thermal displacement result solely from changes in the spatial structure of SST due to heterogeneous warming trends. The fact that the mean warming alters the interannual variability of thermal displacement (owing to changes in the mean spatial SST gradients) makes it unique among existing MHW metrics. Future changes in SST variance could also influence thermal displacement, although past analysis of CMIP5 output indicates that significant projected changes in SST variance ( $P < 0.05$  for >50% of models) are mostly limited to high-latitude regions with reduced ice cover under future warming<sup>40</sup>, and these ice-covered regions are excluded from our analysis. Nonetheless, a more in-depth sensitivity analysis could explore thermal displacement changes forced by time-varying output from individual model projections, considering the strengths and weaknesses of each.

We note that for the future period we calculated SST anomalies relative to the future climatology, not the historical climatology. This approach defines MHWs and their associated thermal displacements as disturbances relative to the contemporaneous climate<sup>31</sup>, which differs from studies that define future MHWs relative to a fixed historical baseline<sup>9,10</sup>. In the context of thermal displacement, the two approaches (that is, using historical versus contemporaneous baselines) provide different information. If one defines displacements relative to a historical baseline, the analysis includes long-term shifts due to the mean warming trend, as well as short-term displacements due to higher-frequency (interannual) variability. The long-term shift is certainly important and has been the focus of the well established literature on climate velocity and its relation to marine species distributions<sup>13–17</sup>. The higher-frequency variability is where we make a novel contribution, focusing on changes in thermal displacement relative to long-term shifts, which are also important from physical and ecological perspectives (see section ‘Justification for MHW definition and implications for this study’).

### Statistics

As is often the case for datasets with lower boundaries, MHW metrics, including intensity and thermal displacement, are skewed to the right (Extended Data Fig. 1), with a long right tail made up of events that are especially intense or generate especially large displacements. Given the skewness of the distributions, we characterize them using medians, percentiles and interquartile ranges instead of means and standard deviations. Where spatial correlations are reported, they represent the Spearman rank correlation coefficient ( $r$ ) calculated across all ocean areas without ice cover. In total, ~500,000 grid points are used for these correlations, but the number of effective degrees of freedom is much lower owing to spatial autocorrelation in the SST and MHW fields (for example, in Figs. 1a, c, 2a). The spatial decorrelation scales of these fields are highly variable in space (for example, they are lower in coastal regions and dynamic current systems), which complicates the accurate determination of the effective degrees of freedom. As a result, we refrain from reporting the significance of spatial correlations; however, we can safely say that the stronger correlation coefficient that

# Article

we report ( $r = -0.81$ ) is significant, as it would require only -15 effective degrees of freedom, whereas the weaker correlation ( $r = -0.27$ ), even if significant, indicates negligible correspondence between the two variables (~7% shared variance). For temporal correlations in a given location (Extended Data Fig. 4), each MHW is assumed to be statistically independent.

## Justification for MHW definition and implications for this study

Here we discuss the justifications for using monthly data and detrending SST anomalies, and the implications of those choices for the results of the study. We note at the outset that they do not qualitatively affect our findings; using monthly instead of daily data alters the frequency and duration of identified MHWs (Extended Data Table 1, Extended Data Fig. 6), but MHW intensities are only slightly reduced and impacts on thermal displacements are negligible (Extended Data Table 1, Extended Data Fig. 7). Similarly, using a fixed 1982–2011 baseline climatology instead of detrending the historical SST data generally increases MHW intensities and thermal displacements, most notably in the high northern latitudes, but produces no consequential changes in our conclusions (Extended Data Figs. 8–10).

The recommended MHW definition of Hobday et al.<sup>21</sup> has been adopted by many in general terms, although details of the methodology have been altered depending on the particular aims and constraints of different studies. For example, Holbrook et al.<sup>11</sup> used the 98th percentile as a threshold (instead of the 90th percentile) because “a 90th percentile threshold resulted in too many small events that made it unclear when the main event was taking place”. Using monthly instead of daily data similarly limits identified MHWs to the ‘main events’. Data with monthly resolution and/or coarse spatial resolution have been used for historical analyses and future projections<sup>9,10,41</sup>, and monthly data are used in forecasts for MHWs and other SST anomalies<sup>42–44</sup>. With respect to the reference period for defining MHWs, several analyses of long-term MHW trends have used fixed baselines<sup>9,10</sup>, although other studies have employed detrended anomalies<sup>11,41</sup> (we note that these studies using fixed baselines and detrended anomalies share many of the same authors). Thus, modifying the Hobday et al.<sup>21</sup> definition is not without precedent; it is a proposal rather than a consensus and indeed the authors state “these metrics can, of course, be modified to suit the specific application”. Below we outline the justifications for our choices in the context of this study, addressing first the use of the monthly data and then the removal of long-term warming trends.

We chose to use monthly SST data for our analysis for several reasons. (i) The atmospheric heatwave definition requires a minimum three-day event duration<sup>21</sup>; although Hobday et al.<sup>21</sup> note that for MHWs “minor differences to the atmospheric definition (minimum duration and minimum time between events) were implemented because of the naturally longer time scales of ocean variability compared with atmospheric variability”, the adjustment from three days for the atmosphere to five days for the ocean is not representative of their different scales of variability. The atmosphere has very little memory and is often treated as stochastic, whereas decorrelation timescales in the ocean can range from days to over a year (see ref. <sup>45</sup> and references therein). Thus, we argue that a minimum MHW duration of a month represents a more appropriate scaling relative to the atmospheric heatwave definition. (ii) MHW definitions based on monthly data are more consistent with reported impacts. The MHWs identified as being the most impactful historically have, with few exceptions, lasted at least a month<sup>46,47</sup>, and although MHWs are generally thought of as rare events, according to daily definitions they happen multiple times per year in most locations. For example, in the Eastern Tropical Pacific we find MHWs once every 3–4 years using monthly data, which is consistent with the frequency of El Niño events. By contrast, using daily data with a five-day minimum duration, we find on average 1.2 MHWs per year identified in that region (Extended Data Table 1). (iii) To the extent that thermal displacement can serve as a proxy for distributional shifts of marine species, MHWs

must last long enough for those distributional shifts to occur. Such ecological impacts (for example, marine fishes swimming hundreds or thousands of kilometres) will not be realized in a matter of days. (iv) Thermal displacement calculations are much more computationally expensive than calculations of other MHW metrics (for example, intensity, duration and frequency). In addition to being more appropriate for this analysis for the reasons listed above, the use of monthly data also lowers the computational burden dramatically. Nonetheless, the same methodology can be applied to daily MHW definitions if desired.

There are physical and ecological arguments for detrending SST anomalies when defining and characterizing MHWs in the presence of a long-term warming trend<sup>21</sup>. From a physical perspective, we start from the premise that an MHW is, in fact, a wave (or, more precisely, the warmest part of a temperature anomaly wave). Using a fixed baseline leads to clear violations of wave property definitions (amplitude/intensity, frequency), which are objectively determined relative to a contemporaneous equilibrium position. Furthermore, the proposed qualitative MHW definition of “a discrete prolonged anomalously warm water event”<sup>21</sup> is violated when using a fixed baseline in a warming ocean; eventually historical MHW thresholds are permanently exceeded and MHWs are neither discrete (that is, “with well-defined start and end times”<sup>21</sup>) nor anomalous (given that something that occurs every day is not anomalous).

Arguments in favour of a fixed baseline for MHWs generally invoke impacts on marine species, specifically that (1) they respond to the total temperature change, not just the variability around the mean, and/or (2) they have evolved in response to historical, not future, conditions. We agree with the argument that the total warming is important for species responses, but that does not mean that all warming is associated with MHWs. When changes in temperature due to the combination of MHWs and long-term warming are of interest, metrics such as cumulative stress, degree days or threshold exceedance are appropriate<sup>48</sup>. We also agree with the argument that species have evolved on the basis of past conditions. However, different species respond in different ways, at different thresholds and on different timescales, and their adaptive and evolutionary capacities are similarly disparate in nature and timescale. Thus, although MHW metrics are useful for characterizing marine ecosystem change, no MHW definition will pass the test of being broadly appropriate for marine species responses. As is done for other ecologically important physical ocean phenomena (upwelling for example), MHW metrics should be defined on the basis of physics, and their impacts can then be explored for the organism or application of interest.

Finally, from the perspective of species that have evolved over perhaps millions of years, a 1980–2010 (or similar) baseline has no more relevance than an 1880–1910 or a 2080–2110 baseline. Rather, recent decades offer a useful baseline for us to evaluate the ecosystem because they represent our ‘normal’. Even though the oceans have warmed over the past century, we evaluate MHWs relative to a recent baseline; in the future, people will be similarly interested in variability relative to their ‘normal’. For example, taking the simplifying assumption that a commercial fish species follows surface isotherms, that species will exhibit a relatively slow shift in its mean position due to mean warming, as well as relatively fast shifts around its mean position due to MHWs. The different timescales of the two shifts have different implications for fisheries—the slow shift would dictate changes regarding where fishing operations should be based, whereas the fast shifts would dictate year-to-year disruptions in the fishery. One could think of an analogy using sea level—if a beach has waves that are 1 m high and the sea level rises 2 m owing to warming and ice melt, would we say that the waves are now 3 m high? We argue that that would be technically incorrect and misleading; characterizations of waves and mean sea level rise should be kept separate so that, as appropriate, waves can be assessed separately (for example, by a surfer who cares only about the wave height) or in combination with the mean change (for example, by a beachfront property owner who cares about the total sea level change).

## Data availability

NOAA High Resolution OISSTv2 data were obtained from NOAA/OAR/ESRL PSL, Boulder, Colorado, USA, at <https://www.esrl.noaa.gov/psd/>. CMIP5 outputs were obtained from Earth System Grid Federation (<https://esgf-node.llnl.gov/projects/cmip5/>). The CMIP5 ensemble mean SST fields used in this analysis are available from J.D.S. (james.d.scott@noaa.gov).

## Code availability

All analyses were performed using MATLAB. Codes can be accessed at [https://github.com/mjacox/Thermal\\_Displacement](https://github.com/mjacox/Thermal_Displacement).

38. Reynolds, R. W. et al. Daily high-resolution-blended analyses for sea surface temperature. *J. Clim.* **20**, 5473–5496 (2007).
39. Banzon, V., Smith, T. M., Chin, T. M., Liu, C. & Hankins, W. A long-term record of blended satellite and in situ sea-surface temperature for climate monitoring, modeling and environmental studies. *Earth Syst. Sci. Data* **8**, 165–176 (2016).
40. Alexander, M. A. et al. Projected sea surface temperatures over the 21st century: changes in the mean, variability and extremes for large marine ecosystem regions of Northern Oceans. *Elementa Sci. Anthrop.* **6**, 9 (2018).
41. Scannell, H. A., Pershing, A. J., Alexander, M. A., Thomas, A. C. & Mills, K. E. Frequency of marine heatwaves in the North Atlantic and North Pacific since 1950. *Geophys. Res. Lett.* **43**, 2069–2076 (2016).
42. Hu, Z. Z., Kumar, A., Jha, B., Zhu, J. & Huang, B. Persistence and predictions of the remarkable warm anomaly in the northeastern Pacific Ocean during 2014–16. *J. Clim.* **30**, 689–702 (2017).
43. Doi, T., Behera, S. K. & Yamagata, T. Merits of a 108-member ensemble system in ENSO and IOD predictions. *J. Clim.* **32**, 957–972 (2019).

44. Jacox, M., Tommasi, D., Alexander, M., Hervieux, G. & Stock, C. Predicting the evolution of the 2014–16 California Current System marine heatwave from an ensemble of coupled global climate forecasts. *Front. Mar. Sci.* **6**, 497 (2019).
45. Romanou, A., Rossow, W. B. & Chou, S. H. Decorrelation scales of high-resolution turbulent fluxes at the ocean surface and a method to fill in gaps in satellite data products. *J. Clim.* **19**, 3378–3393 (2006).
46. Hobday, A. J. et al. Categorizing and naming marine heatwaves. *Oceanography* **31**, 162–173 (2018).
47. Frölicher, T. L. & Laufkötter, C. Emerging risks from marine heat waves. *Nat. Commun.* **9**, 650 (2018).
48. Diffenbaugh, N. S. & Ashfaq, M. Intensification of hot extremes in the United States. *Geophys. Res. Lett.* **37**, L15701 (2010).

**Acknowledgements** The idea for this study derived from discussions of the NOAA/NMFS Spatial Indicators working group, led by L. Barnett and E. Ward. We thank L. Barnett, C. Harvey, M. Hunsicker and A. O. Shelton for discussions and for comments on an earlier version of the manuscript. This study was supported by funding from the NOAA Climate Program Office's Coastal and Ocean Climate Applications programme, the Modeling, Analysis, Predictions, and Projections programme and the NOAA Fisheries Office of Science and Technology (grants NA17OAR4310268 and NA17OAR4310108).

**Author contributions** M.G.J. conceived the study, performed the heatwave analysis and drafted the manuscript. M.A.A. and S.J.B. contributed to the interpretation and presentation of the results. J.D.S. processed the CMIP5 output. All authors revised the manuscript.

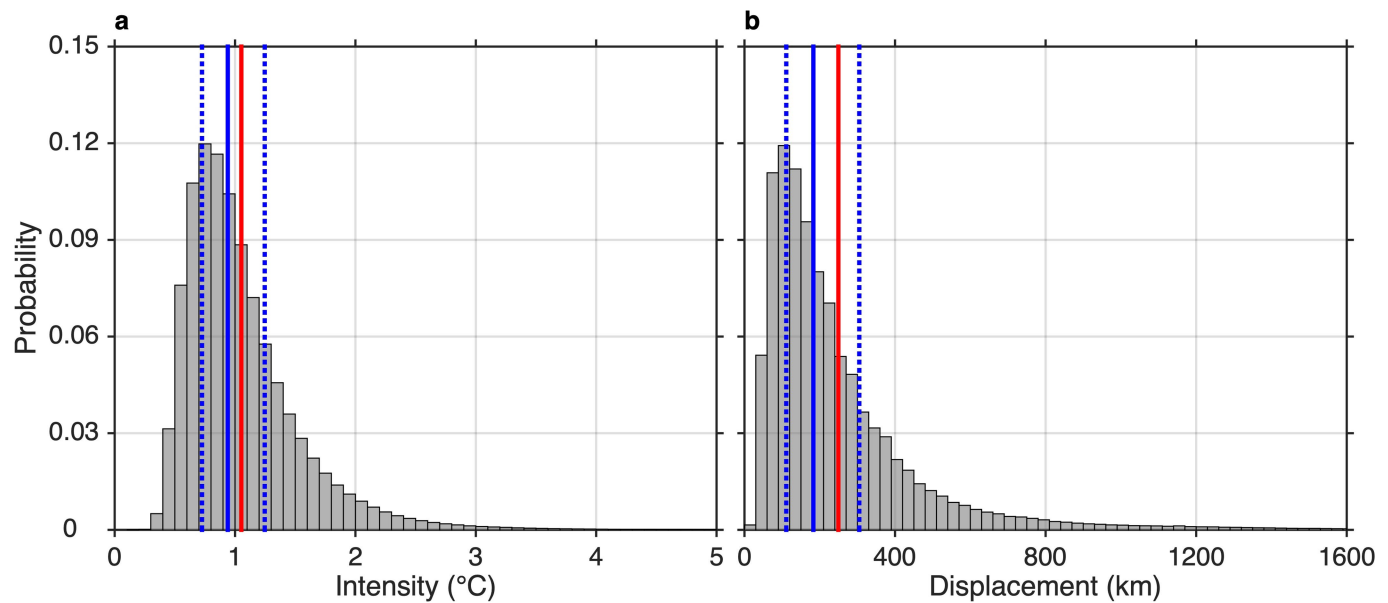
**Competing interests** The authors declare no competing interests.

### Additional information

**Correspondence and requests for materials** should be addressed to M.G.J.

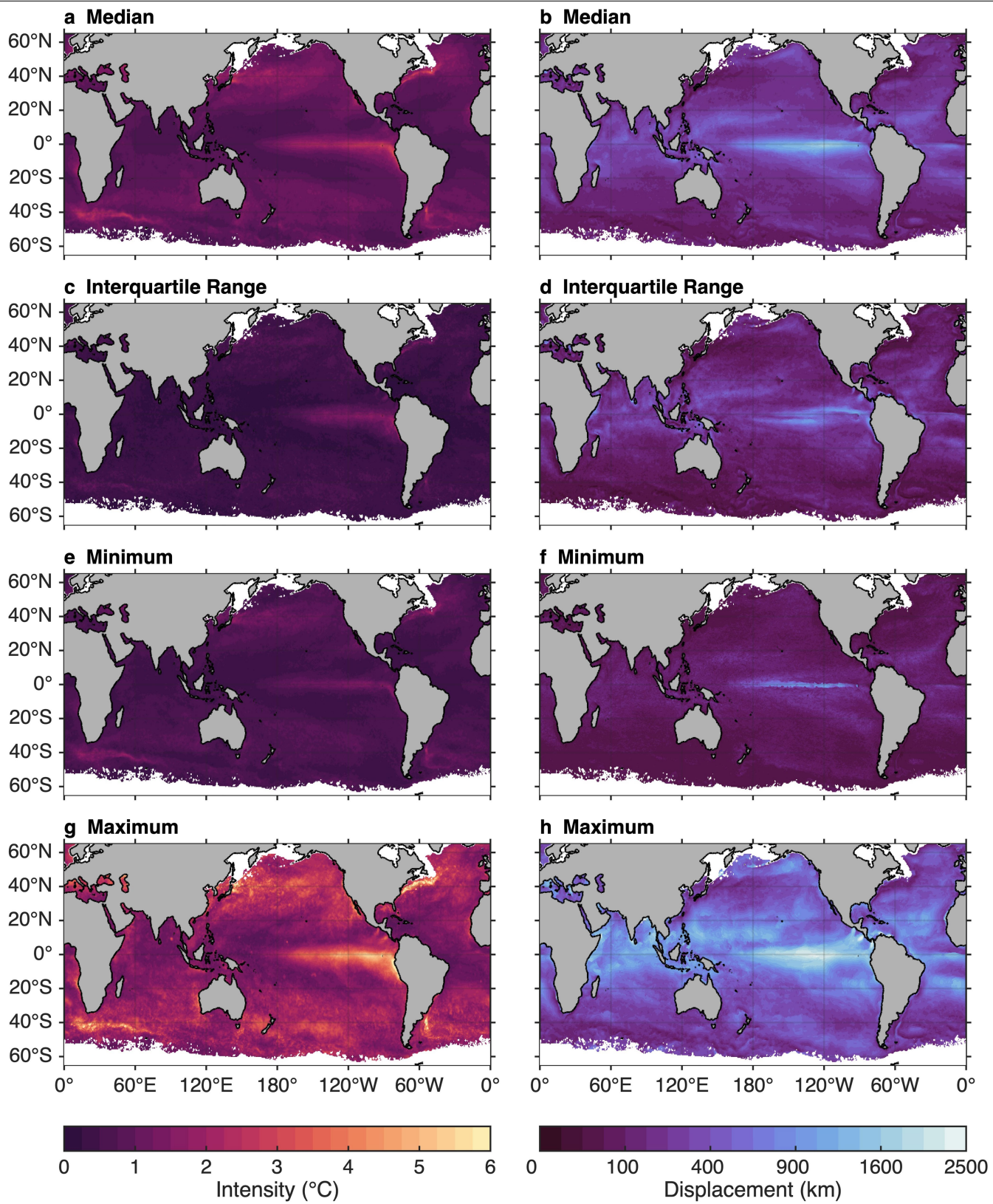
**Peer review information** *Nature* thanks Mark R. Payne, Laurene Pecuchet, Robert Schlegel and the other, anonymous, reviewer(s) for their contribution to the peer review of this work.

**Reprints and permissions information** is available at <http://www.nature.com/reprints>.

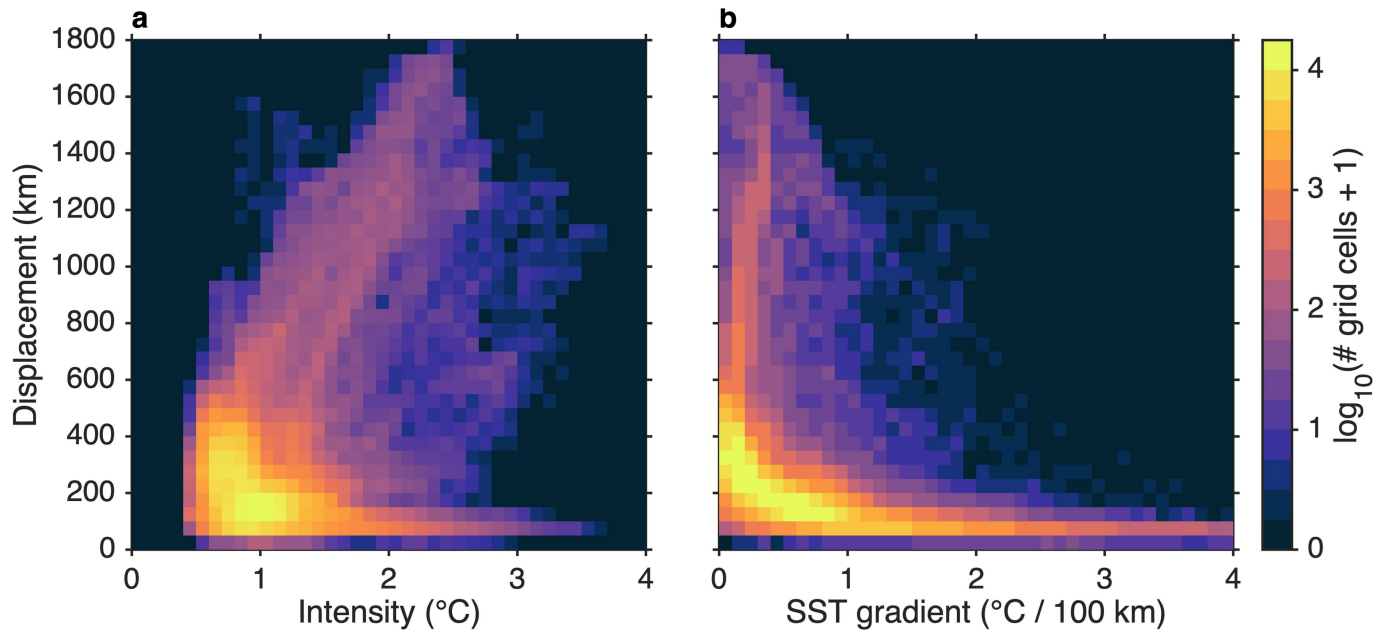


**Extended Data Fig. 1 | Distributions of MHW intensity and thermal displacement.** **a, b,** Histograms of MHW intensity (a) and thermal displacement (b) are shown for months with active MHWs from 1982 to 2019,

aggregated across all OISST grid cells without ice cover. Vertical lines indicate medians (solid blue lines), 25th and 75th percentiles (dashed blue lines) and means (solid red lines) of each distribution.

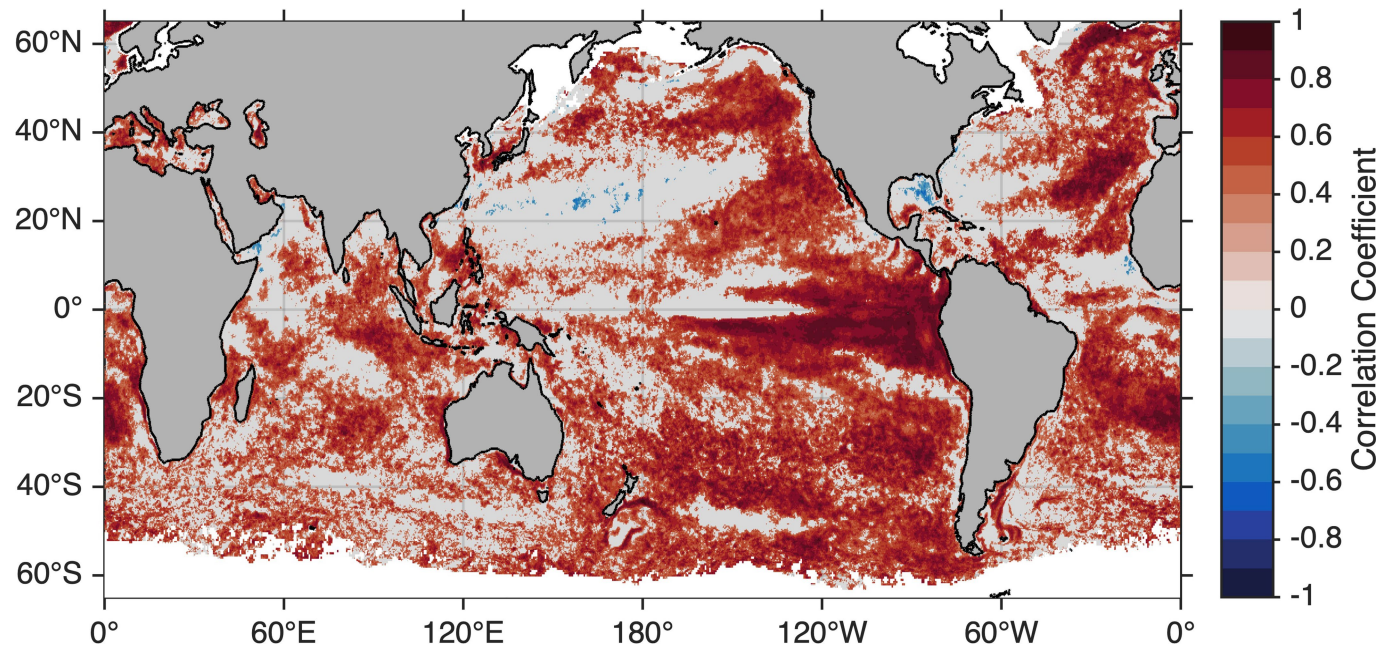


**Extended Data Fig. 2 | Statistics of MHW intensity and thermal displacement.** **a–h**, Median (a, b), 25th–75th percentile range (c, d), minimum (e, f) and maximum (g, h) values of the MHW intensity (a, c, e, g) and thermal displacement (b, d, f, h) calculated across all MHW events from 1982 to 2019.



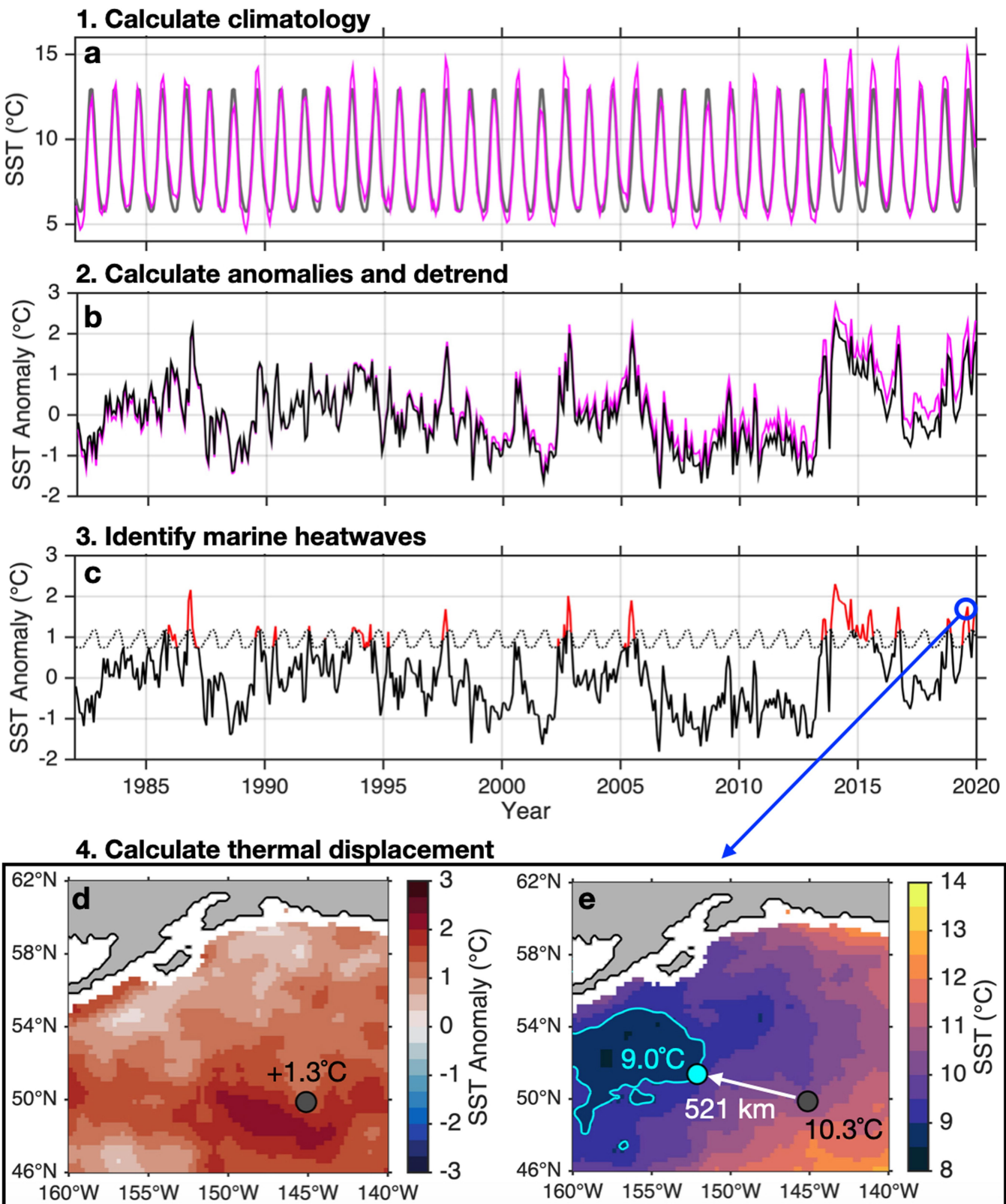
**Extended Data Fig. 3 | Spatial variability in thermal displacement is more dependent on spatial SST gradients than on MHW intensity.** **a, b,** Colours represent the number of  $0.25^{\circ}$  OISST grid cells that fall into each bin of thermal

displacement and MHW intensity (**a**) or SST gradient (**b**). The sum of grid cells in all bins is the total number of ice-free OISST grid cells ( $n \approx 500,000$ ). Spearman rank correlations are  $r = -0.27$  (**a**) and  $r = -0.81$  (**b**).



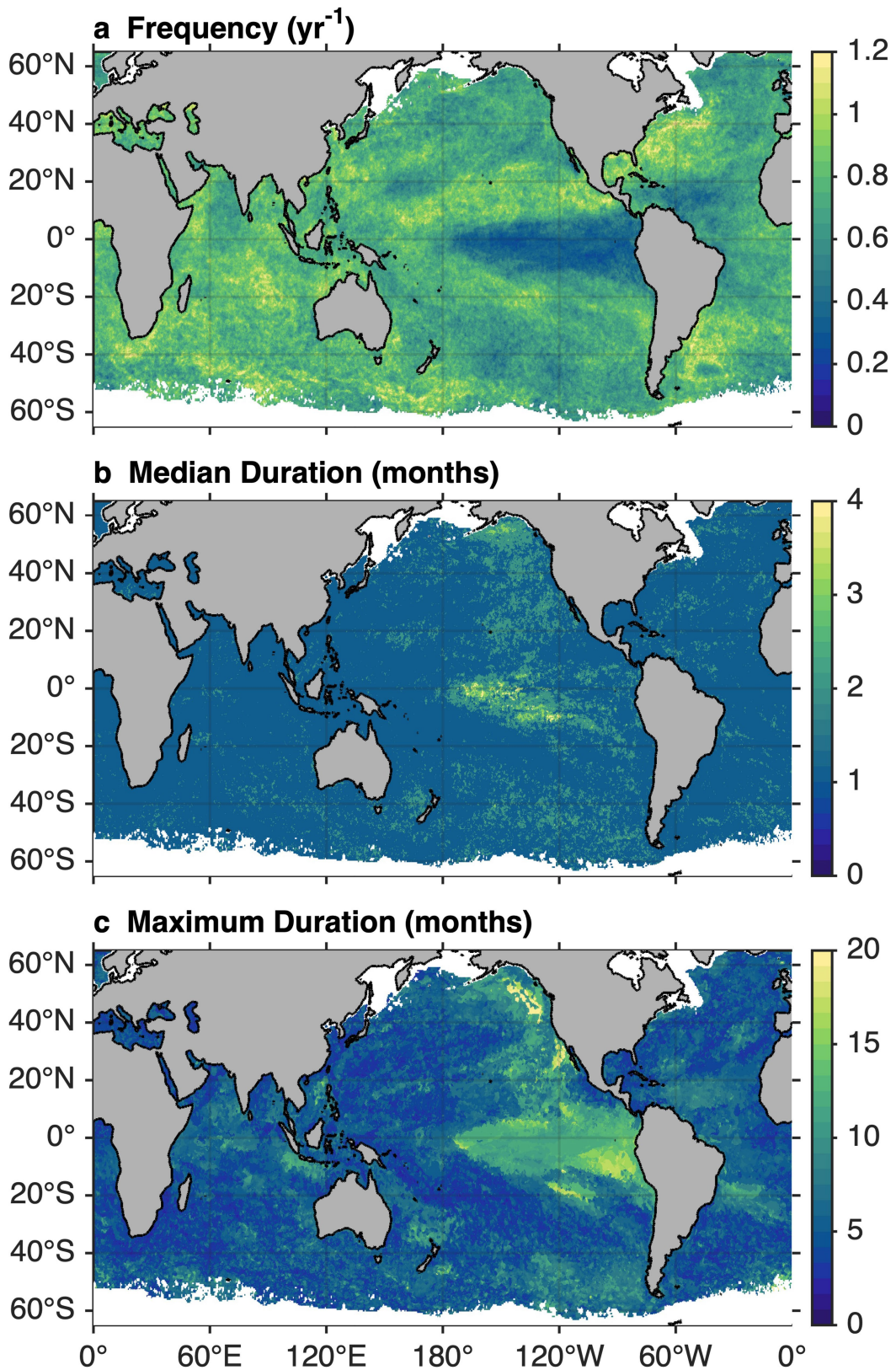
**Extended Data Fig. 4 | Temporal variability in thermal displacement is dependent on MHW intensity for much of the global ocean.** Spearman rank correlation coefficients between MHW intensity and thermal displacement are

shown for each grid cell. Locations where correlations are insignificant at the 95% significance level are greyed out. Significance calculations assume that each MHW event in a given location is statistically independent.



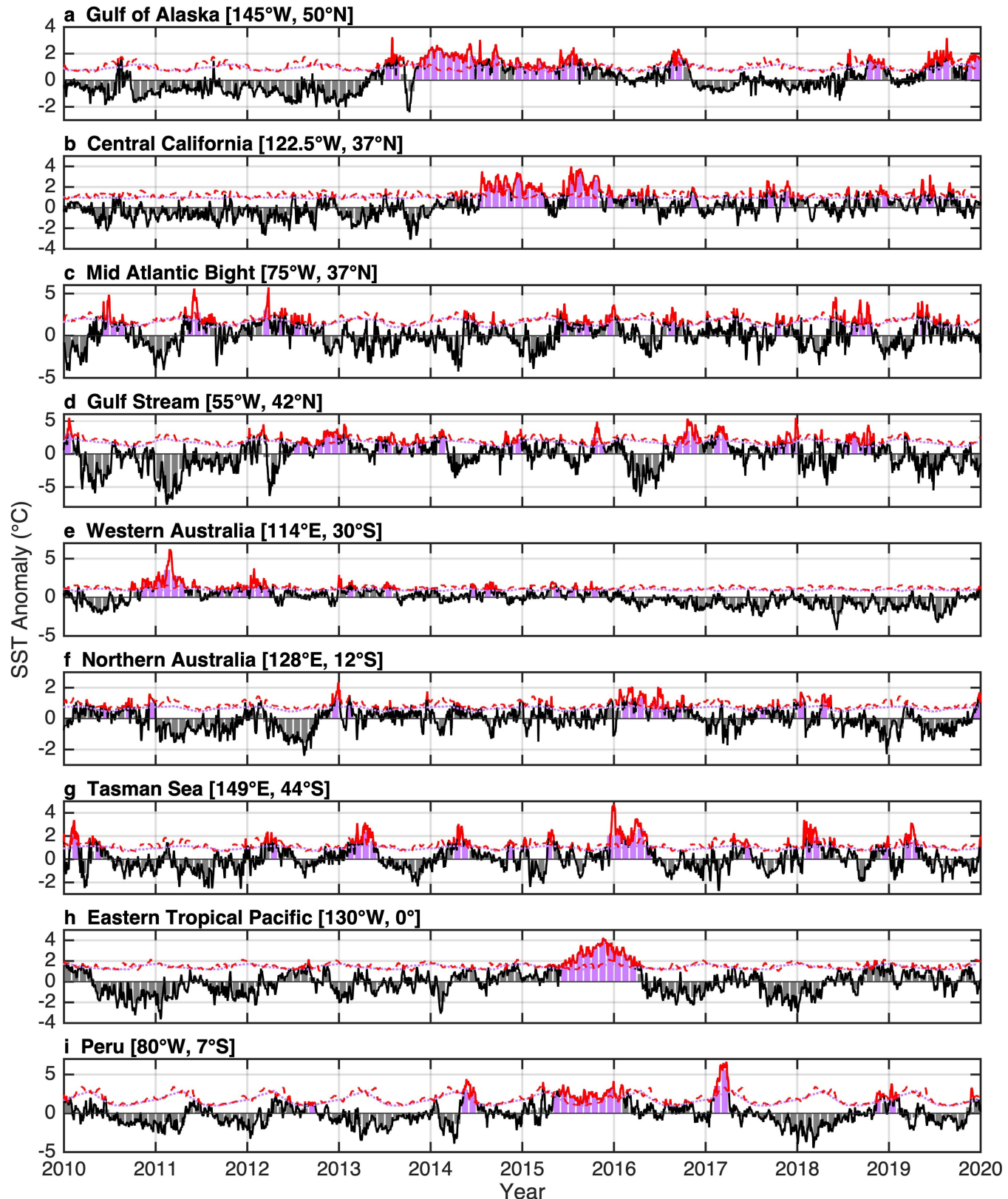
**Extended Data Fig. 5 | Thermal displacement methodology.** Steps for calculating thermal displacement are illustrated for a sample location in the Gulf of Alaska (145° W, 50° N). For each ice-free grid cell in the global ocean ( $n \approx 500,000$ ), the following steps are taken. **a**, The 1982–2011 monthly climatological temperature (grey) is calculated from the OISSTv2 data (magenta). **b**, The monthly climatology is subtracted to obtain monthly anomalies (magenta), which are then linearly detrended (black). **c**, MHWs (red) are identified as months in which the detrended SST anomaly (black) exceeds a

seasonally varying 90th-percentile threshold (dotted black line). For each month with an MHW occurring (August 2019 is highlighted here for example), the detrended SST anomaly (1.3 °C in this case; **d**) is subtracted from the observed SST (10.3 °C; **e**) to obtain the ‘normal’ temperature for that month of the year corrected for the warming trend (9.0 °C). **e**, Thermal displacement is the shortest distance (521 km; white arrow) to SST at or below the ‘normal’ temperature (cyan contour). For the future projections, the same methodology is used after adding the mean projected SST change to the time series in **a**.



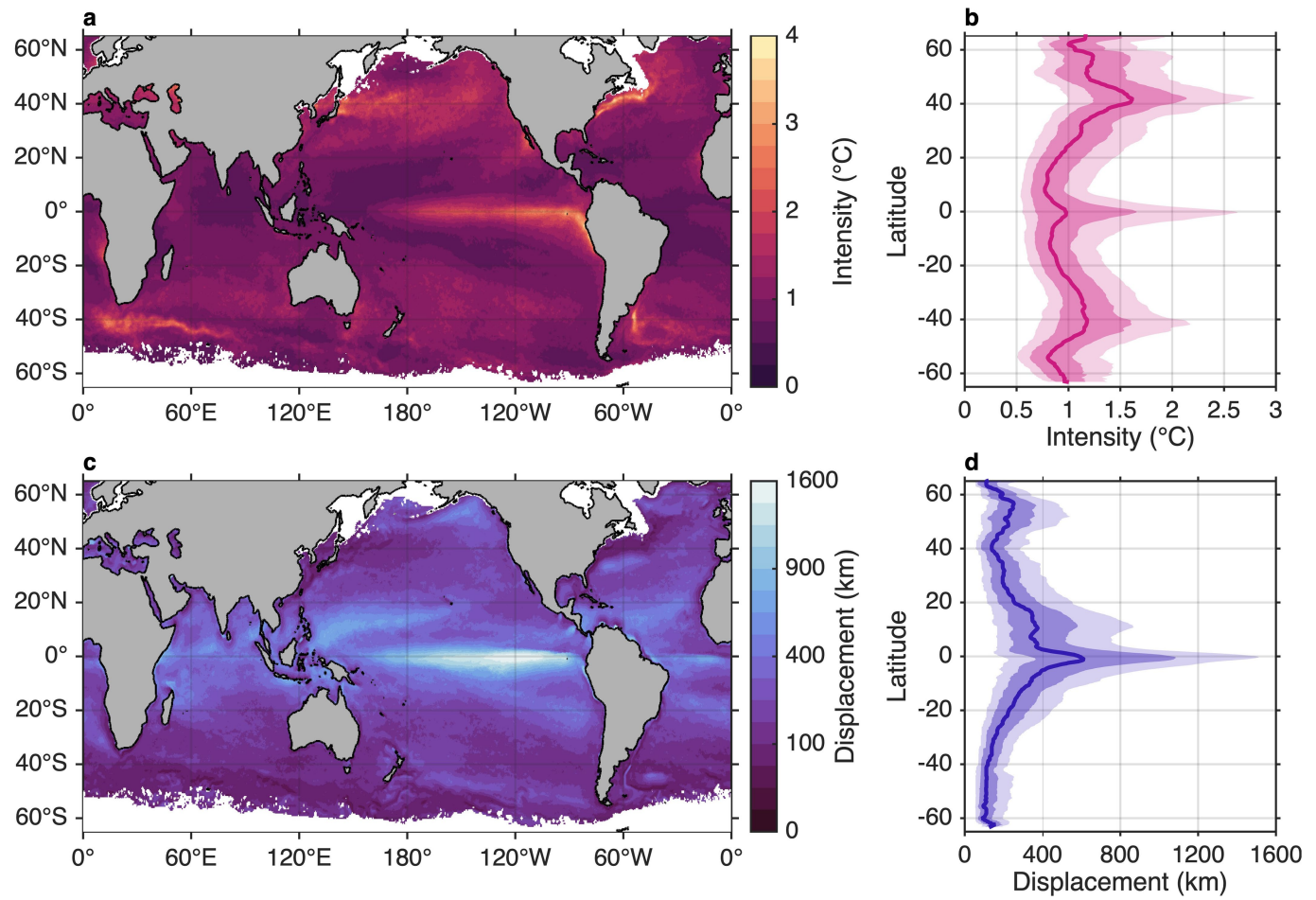
**Extended Data Fig. 6 | Frequency and duration of MHW events.** **a–c**, For each grid cell, MHW frequency (a), median duration (b) and maximum duration (c), calculated from monthly mean SST anomalies, are shown for 1982–2019.

# Article



**Extended Data Fig. 7 | MHW definitions based on daily versus monthly SST data are consistent.** a–i, SST anomaly time series are shown for each of the locations in Fig. 3. Daily data are shown as lines and vertical bars depict monthly data. MHWs defined from the daily data (using a 90th-percentile threshold, a five-day minimum duration and at least two days separating distinct events) are

shown as red lines. MHWs defined from the monthly data (using a 90th-percentile threshold and a one-month minimum duration) are shown as purple bars. The SST anomaly thresholds used to define MHWs in each location are shown as red dashed (daily) and purple dotted (monthly) lines, which are often overlapping.



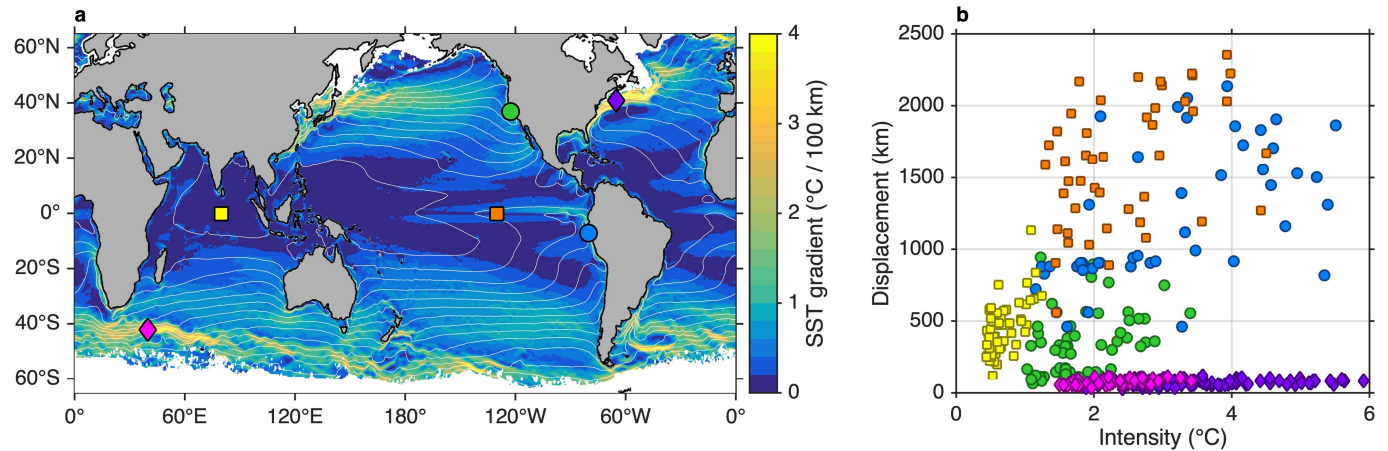
**Extended Data Fig. 8 | Marine heatwaves and their influence on thermal habitat redistribution globally, calculated with a fixed historical baseline.**

**a**, Median MHW intensity (the SST anomaly associated with an MHW) from 1982 to 2019, calculated at each grid cell from all months with an active MHW.

**c**, Median thermal displacement associated with MHWs. Thermal

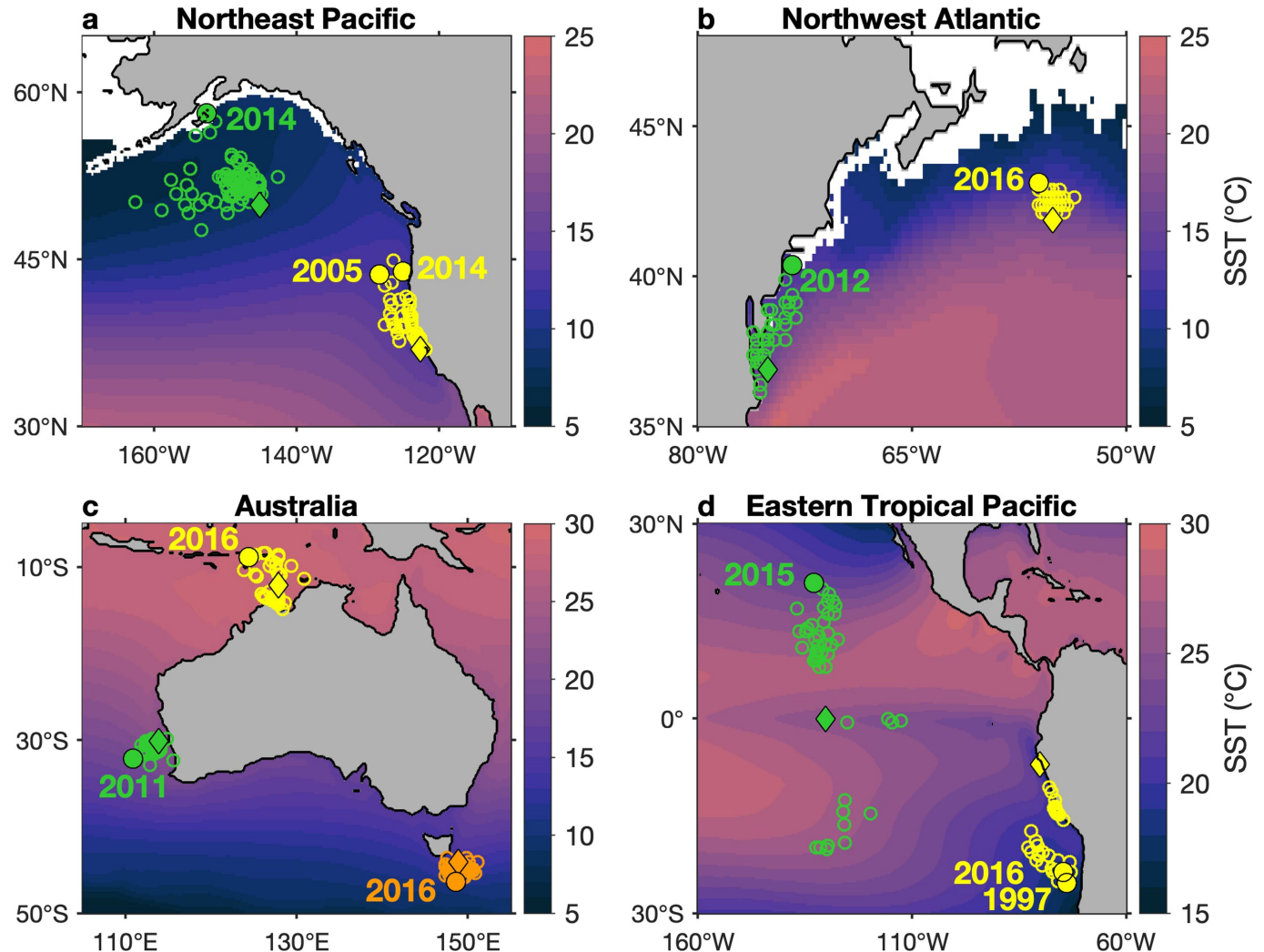
displacements can be in any direction (see Methods). White regions have seasonal or permanent sea ice cover. **b, d**, Zonal median values of MHW intensity and thermal displacement, with bands indicating the 25th–75th and 10th–90th percentile ranges. In contrast to Fig. 1, MHWs here were calculated without detrending SST anomalies relative to the 1982–2011 climatology.

# Article



**Extended Data Fig. 9 | Dependence of thermal displacement on MHW intensity and background SST gradients, calculated with a fixed historical baseline.** **a**, Horizontal SST gradients (colour) and mean SST (contours ranging 2–28 °C at 2 °C intervals), with sample locations indicated by coloured markers. **b**, Thermal displacement as a function of monthly MHW intensity for all 1982–2019 MHWs in six sample regions, characterized by strong SST gradients

(diamonds; Gulf Stream: purple, Antarctic Circumpolar Current: pink), weak SST gradients (squares; Tropical Indian Ocean: yellow), Eastern Tropical Pacific: orange) and coastal upwelling that provides cold refugia (circles; California Current System: green, Humboldt Current System: blue). In contrast to Fig. 2, MHWs here were calculated without detrending SST anomalies relative to the 1982–2011 climatology.



**Extended Data Fig. 10 | Thermal displacements for select locations subject to notable MHWs, calculated with a fixed historical baseline.** a–d, For each region, displacements from select locations (diamonds) are shown for all months with an active MHW from 1982 to 2019 (open circles). Displacements and years of the most intense MHWs are also shown for each location (filled circles). Spatial scales differ between panels; for reference, displacement distances for labelled events are: in a, 1,039 km (Gulf of Alaska, 2014), 895 km

and 807 km (US West Coast, 2005 and 2014, respectively); in b, 418 km and 161 km (Northwest Atlantic, 2012 and 2016, respectively); in c, 362 km (Western Australia, 2011), 526 km (Northern Australia 2016) and 251 km (Tasman Sea 2016), and in d, 2,354 km (Eastern Tropical Pacific, 2015), 2,135 km and 1,926 km (South American West Coast, 1997 and 2016, respectively). In contrast to Fig. 3, MHWs here were calculated without detrending SST anomalies relative to the 1982–2011 climatology. Background colour indicates 1982–2019 mean SST.

# Article

**Extended Data Table 1 | Influence of monthly averaging on MHW metrics**

Location	Frequency (yr <sup>-1</sup> )		Duration (day)		Intensity (°C)		Displacement (km)	
	Daily	Monthly	Daily	Monthly	Daily	Monthly	Daily	Monthly
Gulf of Alaska [145°W, 50°N]	2.0	0.7	12 (6-22)	61 (30-91)	1.6 (1.2-1.9)	1.3 (1.1-1.7)	279 (195-390)	287 (221-413)
Central California [122.5°W, 37°N]	1.8	0.8	9 (7-20)	30 (30-30)	2.0 (1.6-2.4)	1.5 (1.2-2.1)	273 (146-452)	273 (120-392)
Mid Atlantic Bight [75°W, 37°N]	2.7	0.8	8 (6-12)	30 (30-61)	2.4 (2.0-3.2)	1.9 (1.3-2.3)	139 (83-222)	111 (67-165)
Gulf Stream [55°W, 42°N]	2.8	0.9	8 (6-14)	61 (30-61)	2.8 (2.3-3.3)	2.1 (1.7-2.8)	83 (59-104)	83 (56-93)
Western Australia [114°E, 30°S]	2.0	0.7	7 (5-14)	30 (30-61)	1.7 (1.4-2.0)	1.3 (1.1-1.5)	114 (87-177)	114 (83-156)
Northern Australia [128°E, 12°S]	2.1	0.8	7 (5-12)	30 (30-61)	1.3 (1.0-1.6)	0.9 (0.8-1.1)	238 (169-389)	245 (178-424)
Tasman Sea [149°E, 44°S]	2.4	0.9	8 (6-16)	30 (30-61)	1.7 (1.4-2.1)	1.3 (1.1-1.7)	92 (68-118)	85 (74-113)
Eastern Tropical Pacific [130°W, 0°]	1.1	0.3	9 (6-17)	46 (30-213)	2.4 (1.9-3.2)	2.1 (1.6-2.9)	1390 (1133-1866)	1608 (1203-1948)
Peru [80°W, 7°S]	1.0	0.4	8 (6-15)	30 (30-76)	3.3 (2.3-4.6)	3.1 (2.1-4.3)	1105 (858-1538)	954 (861-1634)

For each of the locations in Fig. 3, MHW metrics are shown on the basis of (i) daily SST anomalies used to define MHWs with a 90th-percentile threshold and a five-day minimum duration<sup>21</sup>, and (ii) monthly SST data used to define MHW with a 90th-percentile threshold and a one-month minimum duration. For the duration, intensity and thermal displacement, median values are shown, with the 25th–75th percentile range in parentheses.